Origin of quasiperiodic dynamics in excitable media

Ira B. Schwartz* and Ioana Triandaf
Naval Research Laboratory, Special Project in Nonlinear Science, Code 6700.3, PPD, Washington, D.C. 20375

Joseph M. Starobin
University of North Carolina, Greensboro, North Carolina 27402

Yuri B. Chernyak
Massachussetts Institute of Technology, Room E25-35, Cambridge, Massachusetts 02139
(Received 13 April 1999; revised manuscript received 3 February 2000)

Analysis of the dynamic instabilities of periodic waves in a one-dimensional excitable ring medium demonstrates that driven oscillations of a pulse width display different oscillatory behavior at different values of stimulation frequency. Initial periodicity evolves to quasiperiodic dynamics when the propagation speed of a pulse approaches its minimal value determined by the dispersion relation of a medium.

PACS number(s): 82.40.Bj, 05.45.Pq

Studies of complex dynamics in excitable media are the subject of significant theoretical and practical importance [1–3]. Complex dynamics is known to be related to a broad range of aperiodic phenomena in chemical and biological excitable media [4] and may provide a mechanism for cardiac fibrillation, for example [5,6]. Experimental data [7] and clinical observations of chaotic dynamics [8] may be interpretted as a quasiperiodic (QP) transition to chaos in excitable media, a mechanism introduced by Ruelle and Takens [9]. Unlike a period-doubling route to chaotic behavior, the Ruelle–Takens result predicts complex or chaotic behavior in systems having three independent characteristic frequencies [9]. However, the underlying origin of such frequencies which lead to QP dynamics in excitable media is unclear.

In this brief report we show how QP behavior appears from periodic perturbations of a periodic wave represented as a pulse circulating in a one-dimensional ring of an excitable medium. In this case the length L of the ring is equal to the wavelength of a steady-state periodic (unperturbed) wave train. It represents a major spatial scale which fully determines the system's periodic dynamics (steady circulation) via the dispersion relation for the medium. A single perturbation of a steadily circulating stable pulse results in damped oscillations of its width and velocity (eigenoscillations). We demonstrate quasiperiodicity for driven circulation of a pulse in a ring for the simplest increasing monotonic dispersion curve, and show that it occurs only if the eigenoscillations damp relatively slow. Specifically, quasiperiodicity develops only in the presence of three independent oscillatory processes: the steady-state circulation of a pulse, the (almost) undamped oscillations of its width and velocity, and the external pacing.

We locally stimulate the ring periodically. These periodic perturbations initiate three nonlinearly interacting oscillatory dynamic processes. The first process is specified by a frequency of the steady-state circulation of a pulse f_{ss}, the second by the frequency of the pulse width eigenoscillations f_{eig}, and finally the third one by the stimulation frequency f_s. We controlled the wavelength L varying it from large wavelengths down to its minimal value L_{min}, near which the eigenoscillations are long lived and below which a periodic wave dies [10]. We found that when L is near L_{min}, even insignificant variations of stimulation frequency $\Delta f_s \equiv |f_s - f_{ss}|$, within the range determined by the inequality $\Delta f_s / f_{ss} < 1$, cause the transition from periodic phase-locked regimes reported in [7] to complex QP dynamics.

To carry out our simulations in the correct region of the dispersion curve, we need a reaction–diffusion system for which the dispersion curve and the unperturbed periodic dynamics can be described analytically. Such a model is provided by an exactly solvable model, namely [11]

$$\frac{\partial}{\partial t}u(x,t) - \frac{\partial^2}{\partial x^2}u(x,t) = -i(u,v,\lambda), \tag{1a}$$

$$\frac{\partial}{\partial t}v(x,t) = \varepsilon[\zeta u(x,t) + v_r - v(x,t)], \tag{1b}$$

$$i(u,v,\lambda) = \begin{cases} \lambda u, & u < v \\ u-1, & v < u. \end{cases} \tag{1c}$$

Here v has the meaning of a dynamically varying excitation threshold with the ground (resting) state value v_r. The excitability of the medium is primarily controlled by constants v_r, and the recovery rate for the variable v, ε. The parameter ζ characterizes the effect of the u variable on v. Since u quickly approaches unity in the wave's front, the product $\varepsilon\zeta$ determines the growth rate of the v wave's leading edge, while ε alone characterizes its falloff on the trailing edge. Finally, the constant λ represents a local relaxation rate for the u variable. Without loss of generality we assume $0 < \lambda < 1$, and choose $u = 0$ and $u = 1$ to be the ground (resting) and excited states of a medium, respectively.

*Present address: Naval Research Laboratory, Center for Biological Science and Engineering, Code 6900.IS, Washington, D.C. 20375.

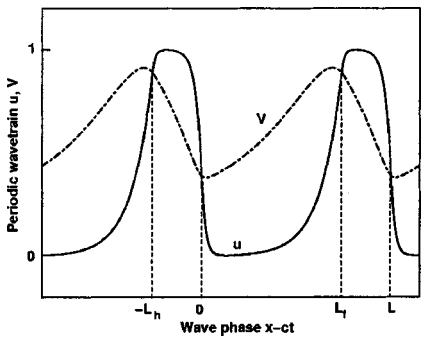

FIG. 1. A snapshot of a periodic steady-state wave-train, u, v for $c=0.85$ at $v_r=0.22$, $\lambda=0.2$, $\zeta=1.2$, and $\varepsilon=0.05$. The values of L_f, L_h, and $L=L_f+L_h$ are marked.

A periodic solution of Eq. (1) is found analytically within ε_1, where $\varepsilon_1=e^{-1/\varepsilon}$ is a new small parameter. The stationary propagating wave-train is characterized by the length L_h of the excited region, in which $u>v$, and the length L_f of the unexcited region, in which $u<v$ (see Fig. 1). The analytical solution yields the widths as explicit functions $L_h(c)$ and $L_f(c)$ of the wave-train propagation speed c found in [12]. These two lengths sum to the spatial period L of the periodic wave-train and determine the dispersion relation for the excitable medium: $L=L_h(c)+L_f(c)$.

First, we explore the evolution of the initially perturbed pulse in the ring and study arising free oscillatory patterns. The initial conditions for Eqs. (1) are chosen as slightly perturbed analytical periodic solutions found in [12]. The perturbation was introduced by cutting off the tail of the wave, i.e., taking the ring's length L slightly smaller than the initial wavelength $L_{\rm init}$. We carried out our simulations along the dispersion curve at a fixed perturbation quasiamplitude: $\chi \equiv (L_{\rm init}(c)-L)/L$, with $L_{\rm init}$ always being greater than L [10]. We varied χ and L moving along the theoretical dispersion curve $c=c_{\rm th}(L)$ from large wavelengths (near the solitary pulse limit) to the minimum one $L_{\rm min}$ at which the oscillations become unstable (the damping approaches zero) [10]. This is similar to the instability reported in [13]. We thus determine the wavelength region in which the forced dynamics may show complex behavior.

Next, we consider the process generated by periodic stimulation. The variable u is periodically perturbed by setting its values to unity at the first seven grid points during one time step per pacing period (the total number of grid points $M=180$). The observed dynamics is determined by the interaction of three periodic processes with three different characteristic periods: the stimulation period $T_s=1/f_s$, the period of the steady-state pulse circulation $T_{\rm ss}=1/f_{\rm ss}$, and the eigenoscillation's period $T_{\rm eig}=1/f_{\rm eig}$. (The period $T_{\rm eig}$ is measured in the numerical experiments without stimulation.) Figure 2 illustrates the driven oscillations of the wave head width L_h for a large ring's length $L=50$ far away from the value $L_{\rm min}=20.04$. In order to have eigenoscillations present from the the outset, we start from a moderately perturbed initial condition determined by $\chi=0.1$. Panel A ($T_s/T_{\rm ss}=0.98$) depicts an incremental transition to periodic phase-locking-like oscillations which correspond to soft excitation scenario [6]. Panel B ($T_s/T_{\rm ss}=1.04$) also shows the incremental oscillations which look similar to those of a linear oscillator under periodic forcing, but additionally incorporate alternating substructures. The behaviors illustrated in these panels are characteristic for the region of the ring lengths far away from $L_{\rm min}$, when the eigenoscillations of L_h quickly damp as shown in panel C. Varying the stimulation period does not result in significant alteration of the stationary oscillatory regimes for sufficiently short T_s. Further decrease of T_s does not change the dynamics which still transitions to strictly periodic patterns. We then decreased the ring length L moving along the theoretical dispersion curve and used the initial conditions corresponding to a very small fixed perturbation quasiamplitude $\chi=0.005$ (The parameter values typically were $\varepsilon=0.1$, $v_r=0.22$, $\zeta=1.2$, $\lambda=0.2$, and $L_{\rm min}=19.87$.) When we reached $L=21.27$ and the damping of the eigenoscillations became very small, we observed that

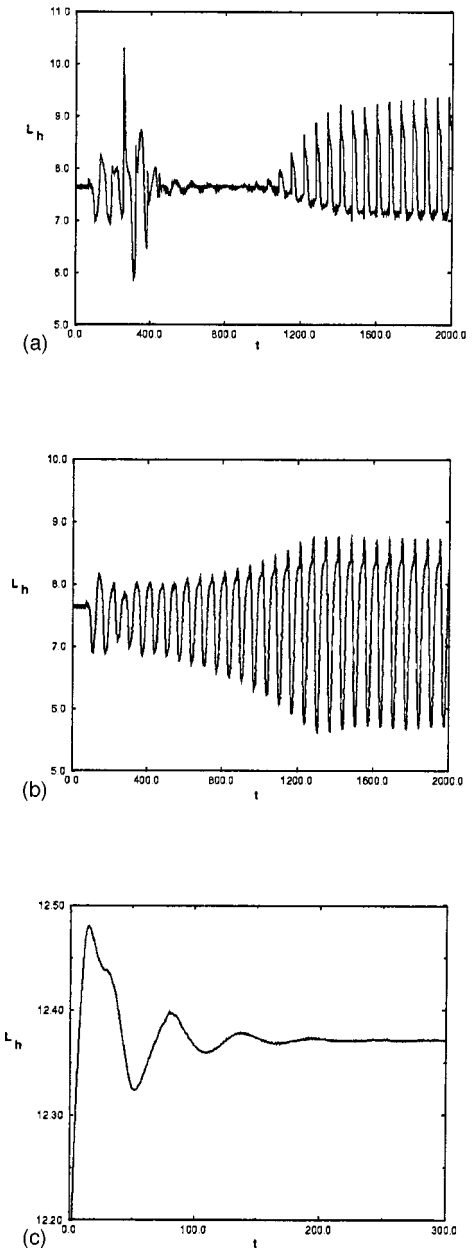

FIG. 2. Driven time oscillations of L_h vs stimulation period T_s: (a) $T_S/T_{\rm ss}=0.98$; (b) $T_S/T_{\rm ss}=1.04$; (c) Rapidly damped eigenoscillations. Parameters are $\lambda=0.4$, $\zeta=1.2$, $\varepsilon=0.02$, $v_r=0.2$, $L=50.0$, and $\chi=0.1$.

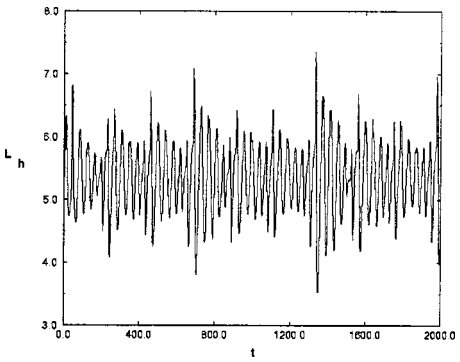

FIG. 3. Complex time series of L_H at $L=21.27$. The stimulation period is $T_s=38.0$.

stimulations of the ring with different periods result in significant changes in the dynamics of oscillations which became fairly complex, as shown in Fig. 3.

In analyzing solutions of Eqs. (1), we assume for a spatial discretization that $u_j(t)=u(x_j,t)$, and $v_j(t)=v(x_j,t)$, where $j=0\ldots M$, and M is the number of spatial mesh points. Periodic boundary conditions are applied at $j=0$ and $j=M$. This results in the system of ordinary differential equations of order $2M+2$.

When computing Lyapunov exponents, it is not sufficient to compute them from a measured time series: as shown in [14], even low dimensional systems may possess spurious maximum Lyapunov exponents. To do the computations properly, one needs to generate the linear variational equations along a solution, and look at the average length of a small vector for a sufficiently long time along the attractor. Since the current system of Eqs. (1) corresponds to a discontinuous vector field, we smooth it by substituting for the function i in Eq. (1c) the following:

$$h(m,x)=\frac{\arctan(mx)}{\pi}+\frac{1}{2}, \tag{2a}$$

$$i(u,v,\lambda)=\lambda u h(m,v-u)+(u-1)h(m,u-v), \tag{2b}$$

Equations (1a), (1b), and (2) allow one to generate a smooth Jacobian without modifying the qualitative behavior of the original discontinuous dynamics, for m sufficiently large.

We consider a localized periodic stimulus S given by an approximate delta function

$$S(t,\omega,\sigma)=e^{-(\sin^2(\omega t/2)/\sigma^2)}, \tag{3}$$

applied over N spatial nodal points (i.e., $j=1,N$), where $N \ll M$. We fix the following parameters so that we are near the minimum length scale of the dispersion curve: $M=180$, $\lambda=0.2$, $\zeta=1.2$, $v_r=0.22$, $\varepsilon=0.1$, $N=7$. The period of the pulse, $T_s=2\pi/\omega$, is our control parameter. The terms corresponding to stimulation at N spatial points are added to the right-hand side of Eq. (1a).

Since the local stimulus is applied periodically, we sample the field $u_j(t_n)$ where $t_n=nT_s$. In this way we generate a Poincare map of the attractor, and perform the following numerical experiment. We fix the period T_s and remove transient behavior. We then compute the next 200

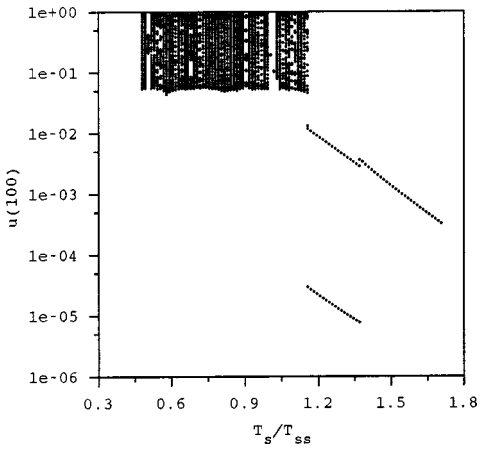

FIG. 4. Bifurcation picture as a function of stimulation period. The solution is a component of u away from the location of the stimulus. The solution is sampled every stimulus period. Here $T_{ss}=32$.

iterates which lie on the attractor. The final values of the vector field are then used as initial data for the next value of the period $T_s+\delta$, where δ is small. The process is then repeated to generate a range of attractors as a function of stimulation period. The results are plotted in Fig. 4, where the solution u_{100} is the component plotted.

There are three major regions of interest in Fig. 4. The first is that for long enough periods, the response is a period one attractor. As period is decreased, the period one undergoes a flip bifurcation to a period two branch. Notice that the amplitude of u of one of the iterates is very small compared to the other amplitude. These small amplitude period two cycles possibly correspond to cardiac alternans [15], which have been conjectured to form spiral breakdown in higher spatial dimensions [16].

As the period of simulation is further decreased, there is another region that appears abruptly in which the period two cycle destabilizes, resulting in a QP attractor. Further detailed computations show that this instability is indeed discontinuous. This QP region consists of both QP and periodic attractors, and does not exhibit chaos in the present model due to the monotonic nature of the dispersion curve, as con-

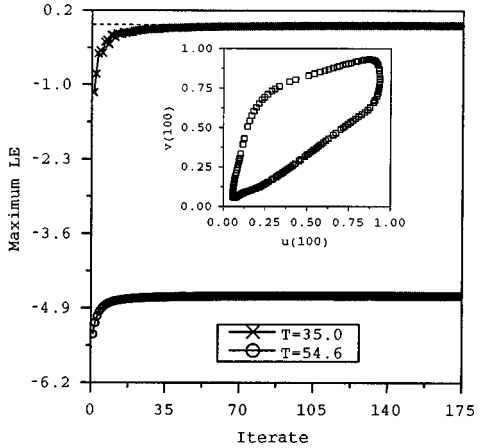

FIG. 5. Maximum Lyapunov exponents for periodic and quasiperiodic cases. The dashed horizontal line denotes an exponent of zero. The inset shows an invariant torus for quasiperiodic motion.

jectured in [17]. For a fixed period in the quasiperiodic regime we show an example of the attractor at $T_s = 35.0$ sampled at the stimulation is shown in Fig. 5 as an invariant torus. In Fig. 5 are plotted the results of computing the maximum Lyapunov exponents as a function of time for the QP attractor at $T_s = 35.0$ as well as the maximal exponent of the periodic attractor at period $T_s = 54.6$. Notice that the periodic attractor has a negative maximum exponent, while that of the QP attractor converges to zero.

We summarize by noting that: (1) The dispersion curve explicitly determines the three frequencies which generate the QP attractors. (2) Near the minimum length scale of the dispersion curve: (a) long periodic stimulation damps out one frequency, implying the existence of periodic attractors only; (b) shorter stimulation periods exciting weakly damped frequencies imply QP attractors are sustained.

This work was supported by the Office of Naval Research, DARPA, Whitaker Foundation Grant No. 96-0161, and NASA Grant No. NAG5-4989.

[1] M. Cross and P. C. Hohenberg, Rev. Mod. Phys. **65**, 851 (1993).
[2] I. Triandaf and I. B. Schwartz, Phys. Rev. E **56**, 204 (1997).
[3] T. J. Lewis and M. R. Guevara, J. Theor. Biol. **146**, 407 (1990).
[4] V. Hakim and A. Karma, Phys. Rev. Lett. **79**, 665 (1997); L. Ge, O. Qi V. Petrov, and H. Swinney, *ibid.* **77**, 2105 (1996).
[5] L. Glass, Phys. Today **49**(8), 40 (1996).
[6] L. Glass and M. C. Mackey, *From Clocks to Chaos* (Princeton University Press, Princeton, NJ, 1988).
[7] D. R. Chialvo, R. F. Gilmour, Jr., and J. Jalife, Nature (London) **343**, 653 (1990).
[8] A. Garfinkel *et al.*, J. Clin. Invest. **99**, 305 (1997).
[9] J. M. T. Thompson and H. B. Stewart, *Nonlinear Dynamics and Chaos* (Wiley, Chichester, 1987).
[10] J. M. Starobin, Y. B. Chernyak, and R. J. Cohen in *Proceedings of the 25th Annual Meeting of Computers in Cardiology*, Cleveland, 1998, edited by A. Murray and S. Swiryn (IEEE, New York, 1998), Vol. 25, pp. 365–368.
[11] Y. B. Chernyak, J. M. Starobin, and R. J. Cohen, Phys. Rev. Lett. **80**, 5675 (1998).
[12] Y. B. Chernyak, J. M. Starobin, and R. J. Cohen, Phys. Rev. E **58**, 4108 (1998).
[13] M. Countemanche, L. Glass, and J. P. Keener, Phys. Rev. Lett. **70**, 2182 (1993).
[14] T. D. Sauer, J. A. Tempkin, and James A. Yorke, Phys. Rev. Lett. **81**, 4341 (1998); T. D. Sauer and J. A. Yorke (unpublished).
[15] J. M. Smith, E. A. Clancey, C. R. Valery, J. N. Ruskin, and R. J. Cohen, Circ. Res. **77**, 110 (1988).
[16] A. Karma, Chaos **4**, 461 (1994).
[17] Z. Qu, J. N. Weiss, and A. Garfinkel, Phys. Rev. Lett. **78**, 1387 (1997).